

## MIT Open Access Articles

*Reliability Based Factors of Safety for VIV  
Fatigue Using NDP Riser High Mode VIV Tests*

The MIT Faculty has made this article openly available. **Please share** how this access benefits you. Your story matters.

**Citation:** Fontaine, E., H. Marcollo, K. Vandiver, M. Triantafyllou, C. Larsen, M. Tognarelli, Y. Constantinides, and O. Oakley. "Reliability Based Factors of Safety for VIV Fatigue Using NDP Riser High Mode VIV Tests." Volume 7: CFD and VIV; Offshore Geotechnics (2011).

**As Published:** <http://dx.doi.org/10.1115/OMAE2011-49820>

**Publisher:** American Society of Mechanical Engineers

**Persistent URL:** <http://hdl.handle.net/1721.1/109336>

**Version:** Final published version: final published article, as it appeared in a journal, conference proceedings, or other formally published context

**Terms of Use:** Article is made available in accordance with the publisher's policy and may be subject to US copyright law. Please refer to the publisher's site for terms of use.



OMAE2011-49820

## RELIABILITY BASED FACTORS OF SAFETY FOR VIV FATIGUE USING NDP RISER HIGH MODE VIV TESTS

**E. Fontaine**  
AMOG Consulting  
Notting Hill, Victoria, Australia

**H. Marcollo**  
AMOG Consulting  
Notting Hill, Victoria, Australia

**K. Vandiver**  
M.I.T.  
Cambridge, MA, USA

**M. Triantafyllou**  
M.I.T.  
Cambridge, MA, USA

**C. Larsen**  
NTNU  
Trondheim, Norway

**M. Tognarelli**  
BP America Production Co.  
Houston, TX, USA

**Y. Constantinides**  
Chevron  
Houston, TX, USA

**O. Oakley**  
Chevron  
San Ramon, CA, USA

### ABSTRACT

Understanding the level of conservatism in a riser system design for vortex-induced vibration (VIV) fatigue is an important issue for operators. This study represents a demonstration of the calibration methodology to derive consistent values for the Factor of Safety (FoS). The exercise is performed here based on medium scale VIV data and utilizing the most commonly used VIV prediction software by industry. The results emphasize the need for (i) a coherent approach to estimate the FoS to be used and (ii) monitoring/measurement of software improvements as this may increase risk of failure if the influence of such improvements on the FoS is not quantified.

### INTRODUCTION

Understanding the level of conservatism in a riser system design against VIV is an important issue for operators. A significant effort has been made over the last fifteen years by several prestigious universities worldwide to develop new VIV models or improve existing ones and to benchmark VIV software against experiments, see for example the blind predictions of laboratory measurements of VIV of a tensioned riser ([1], [2]). Recent field experiments [3] as well as analyses of full scale data ([4], [5]) have confirmed the complex nature of VIV that was previously observed in laboratory experiments [6] and emphasized the importance of in-line vibrations and super-upper harmonics, in addition to the well-known cross-flow vibrations.

From a practical point of view, it has become obvious that deterministic estimates of full scale riser VIV fatigue life will

always include strong intrinsic uncertainties due to (i) the lack of knowledge of the environmental loadings generating VIV and (ii) the complex nature of the VIV response itself. From a design perspective, the role of the FoS is precisely to ensure a level of reliability by taking into account the uncertainty in the prediction of the resulting fatigue lifetime. Its calibration requires assessing the probability of failure.

Previous attempts to calibrate VIV fatigue FoS have been made using uncertainty distributions derived from engineering judgment and laboratory experiments, see for example [7]. It is important to note here that the uncertainties observed in controlled laboratory experiments are often significantly lower than those observed in the field. On the other hand, the ongoing development in more rigorous VIV software is progressively improving the prediction of VIV motion response. It can be overlooked that reducing the mean (but not the RMS) over-conservatism of software prediction while keeping the FoS constant actually leads to an increase of the probability of failure associated with a given FoS value. Ideally, the value of the FoS should closely relate to the complete statistical accuracy of the prediction of the fatigue lifetime estimate.

State-of-the-art VIV fatigue design programs make the best use of available knowledge, but remain limited for several reasons in their capacity to capture the broad complexity of the phenomenon. In addition to more generic uncertainties with regard to structural capacity, like variations in material properties or S-N curves, much uncertainty is linked to the amount and relevance of data available to understand and characterize VIV itself.

Recent field and lab experiments have confirmed complexities of VIV like in-line vibrations, higher harmonics, intermittent behavior, traveling waves and chaotic sensitivity to small perturbations. These phenomena are only in the very earliest stages of being included, if at all, in VIV fatigue analysis codes.

It is clear that relatively simple estimates of riser VIV fatigue life will always include significant, intrinsic uncertainties, obviating the need to account for them in a rational FoS. This leads to the main objectives of the present study, namely, to provide a rational basis for developing appropriate fatigue FoS for VIV and to demonstrate a benchmarking process on a high-quality controlled experimental dataset. Development of a VIV fatigue FoS can be achieved in a coherent manner within the framework of reliability analysis as in [8]. The proposed methodology for development of VIV fatigue FoS consists of:

- (i) Formulating the limit state function that describes the failure scenario,
- (ii) Identifying and probabilistically characterizing the uncertainties involved in the model,
- (iii) Computing the FoS to reach a prescribed level of structural reliability.

The present study made use of controlled experimental data to assess values of the VIV fatigue FoS to meet a defined level of design conservatism. The experimental data were obtained from high length-to-diameter (L/D) ratio 38m riser model test data performed by the Norwegian Deepwater Program (NDP) [9]. These data are recognized as a high-quality dataset taken under controlled experimental conditions and include bare riser, partially straked and fully straked cases.

## FORMULATION OF THE LIMIT STATE FUNCTION

### Failure criteria

When designing a structure for fatigue, we want to virtually eliminate the risk that the actual (or measured) time to failure, or time at which a prescribed fraction of damage capacity is consumed, will be less than the amount of time predicted in our analysis. Design failure can thus be expressed by the following inequality:

$$T_f^m \leq T_f^p \quad (1)$$

where  $T_f$  is the time for failure and superscripts  $p$  and  $m$  refer to predicted and measured quantities, respectively. The different domains are illustrated in Figure 1 where a constant damage rate over the whole life has been assumed for illustration purposes only. In the examples presented later in this paper, as in reality, damage is monotonically increasing but not, in general, linear with time.

The failure defined by eq. (1) can be rewritten in the form:

$$\dot{D}_{Tref}^p - \dot{D}_{Tref}^m \leq 0 \quad (2)$$

where the dot indicates that the (averaged) damage rate is considered. Within the framework of reliability analysis, the

limit state function is classically defined as  $G = R - S$  where  $R$  refers to the resistance and  $S$  to the loading and the failure criteria is  $G \leq 0$ . In eq. (2), the predicted damage rate is to be interpreted as the resistance (as provided by the design process) while the measured value of the damage rate is to be considered as the (effective) loading. The limit state function therefore reads:

$$G = \dot{D}_{Tref}^p - \dot{D}_{Tref}^m \leq 0 \quad (3)$$

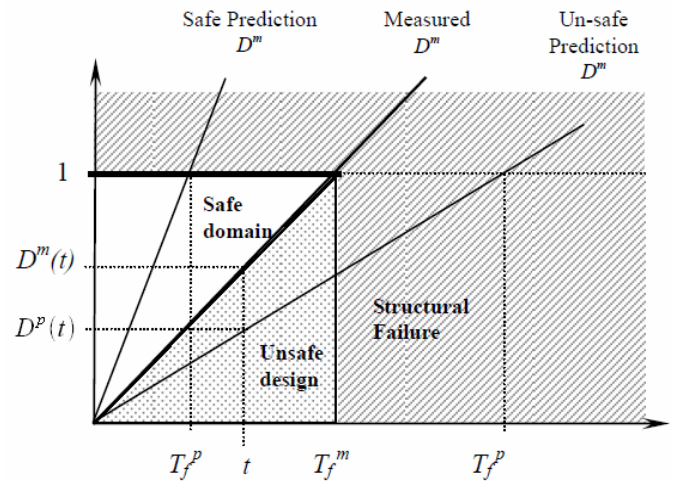


Figure 1: Safe and unsafe design scenarios for VIV fatigue.

### Bias factor

Equation (3) clearly exhibits the role played by the ratio between the predicted value and the measured one. This ratio characterizes the bias factor introduced by the VIV software. Following DNV-F204 [10], the bias factor is defined as:

$$\alpha = \frac{D_{VIV}(\text{Applied Method})}{D_{VIV}(\text{Full Scale Measurements})}$$

The bias factor can be interpreted as the offset from the equality line in Figure 1. With the present notations, the bias factor is defined by:

$$\alpha = \frac{\dot{D}_{Tref}^p}{\dot{D}_{Tref}^m} \quad (4)$$

In this framework,  $\alpha$  is a random variable characterized by its probability distribution. As defined, it describes the whole of the uncertainty associated with the modeling process given a particular predictive model and a particular means of calculating damage rate from measured data.

### Factor of safety

In the context of reliability analysis, the FoS,  $\gamma$ , is introduced by modifying the Limit State Function according to:

$$G = \gamma \cdot \dot{D}_{Tref}^p - \dot{D}_{Tref}^m \quad (5)$$

When the predicted damage multiplied by the FoS is less than the measured damage, then the design is to be considered as unsafe. In other words, the FoS,  $\gamma$  has to be calibrated such that multiplying the predicted damage rate by  $\gamma$  ensures that the associated target level of reliability is reached with respect to the limit state function provided in equation (5). From the reliability analysis, values of  $\gamma$  higher than 1 ( $\gamma > 1$ ) are expected to be found. When a value lower than 1 ( $\gamma < 1$ ) is found, this means that there is so much conservatism involved in the predicted damage that the result can actually be divided by  $1/\gamma$  ( $1/\gamma > 1$ ) to reach the required probability of failure.

### Limit state functions

Using equations (4) and (5), the simplest form of the limit state function is:

$$G = \gamma - \frac{1}{\alpha} \quad (6)$$

where a single loading condition (current profile) has been assumed. The bias factor  $\alpha$  is a random variable while the partial safety factor  $\gamma$  is a deterministic parameter. Though useful for illustration or for checks of singular extreme cases, this particular formulation is not particularly representative in most real design scenarios where we are aggregating the probability-weighted damage due to multiple loading (current) conditions.

Indeed, a more refined expression for the limit state function involves the integral over all the current profiles observed during the period  $T_{ref}$ , or equivalently the probability-weighted summation over all current conditions. As the measured damage is an unknown quantity, it is replaced by its best estimate according to (4). Finally, the complete limit state function reads:

$$G = \gamma \sum_i f_U(u_i) \cdot \dot{D}_U^p(u_i) - \sum_i \frac{1}{\alpha_i} f_U(u_i) \eta \left( \frac{\dot{D}_U^p(u_i)}{\alpha_i} \right) \cdot \dot{D}_U^p(u_i) \quad (7)$$

where the summation is performed over all the current profiles used in the damage prediction,  $f_U(u_i)$  is the probability of occurrence of the current profile and  $\eta$  the measured probability of occurrence of VIV for this current condition, to be derived from experimental measurements, see e.g. [11]. It should be noted here that this formulation is site-specific as it explicitly includes the current profiles and their probability of occurrence.

### Structural reliability

Structural reliability is quantified in the form of probability of failure. The probability of failure in the present context,  $P_f$ , is defined such that:

$$P_f = \Pr[G \leq 0] \quad (8)$$

Knowing the distribution of the bias factor, the direct problem consists of computing the probability of failure for a prescribed value of  $\gamma$ . The inverse problem consists of estimating the

required value of  $\gamma$  for a prescribed failure probability. Both the direct and inverse problem can be solved using First Order Reliability Method – FORM see e.g. [12] – which iteratively computes the design point, the most likely point for which failure will occur, as the limit state function vanishes.

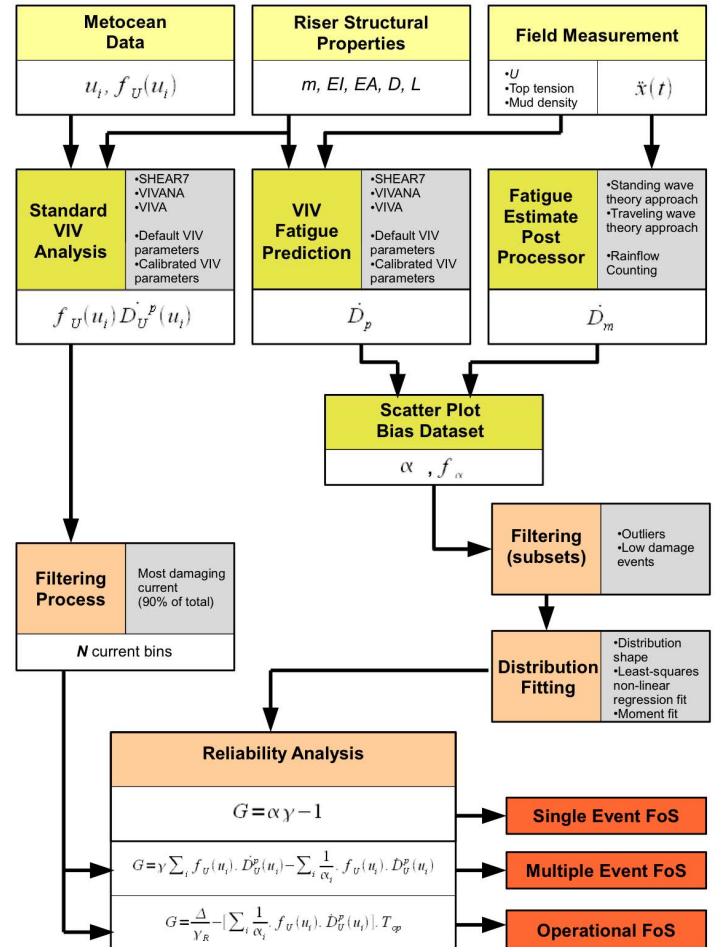


Figure 2 : VIV Fatigue FoS Calibration Methodology

### FOS CALIBRATION METHODOLOGY

The overall methodology of the VIV FoS Calibration, based on previous studies performed, is presented in Figures 2 and 3 and explained hereafter.

- (i) VIV fatigue damage measurements
  - From field measurements or model tests, the bending strain time series on many sensor locations along the riser model were recorded for various current loadings (current speed; uniform / shear current) and riser configurations (bare / partially-straked / fully-straked).
  - The VIV fatigue damage rates corresponding to the various current loadings, riser configurations and locations along the riser model were then derived using a rainflow counting method and an S-N curve assumption.

- Cross-Flow (CF) at the first harmonic only, cross-flow with higher harmonics, or cross-flow and inline vibrations were considered.
- (ii) VIV fatigue damage predictions
- Riser structural models, based on the riser configurations used in model basin or field measurements, were constructed in the VIV prediction software. In the project, three VIV prediction software programs were used: VIVA, SHEAR7 and VIVANA.
  - From model basin or field measurements, the same scenarios (current loadings and riser configurations) were simulated in the VIV prediction software to predict the VIV fatigue damage rates.
  - The predicted VIV fatigue damage rates were then extracted for the same measured locations on the riser.
- (iii) Scatter plots and bias datasets
- Scatter plots of the predicted-versus-measured damage rates were generated. The bias datasets (predictions over measurements) were also derived.
- (iv) Distribution fitting
- Analytical distributions were fitted to the filtered bias datasets. Log-normal, double peak log-normal and kernel based distributions were considered.
- (v) Reliability analysis
- As data points were recorded all along the riser, in locations where high and low damage were measured, the reliability analysis was performed as a function of the damage threshold to assess the sensitivity of the FoS with regard to high/low values of the damage considered in the analysis.
  - Reliability analysis using the simplest limit state function, the single-event limit state function, was performed on each dataset for various damage threshold by means of Monte-Carlo simulation.
  - The FoS values derived are associated with a  $10^{-3}$  probability of failure.

### NDP VIV MODEL TEST EXPERIMENTS

Step (i) of the FoS calibration methodology consists in analyzing measurements of accelerations or strains along the riser undergoing VIV in order to estimate the so-called measured fatigue damage. In the present case, the Norwegian Deepwater Program provided the experimental data. NDP has undertaken an extensive hydrodynamic testing program on a high length-to-diameter ratio ( $L/D$ ) riser. The tests were performed in the MARINTEK Offshore Basin in December 2003. These tests are considered as some of the best available data to study VIV of risers at medium scale in a controlled environment.

A 38m long riser was towed at different speeds, simulating uniform and triangular shear current with intensity (i.e., maximum speed) ranging from 0.3 to 2.4 m/s. The riser was instrumented using 24 strain gauges and 8 accelerometers in the cross-flow direction and 40 strain gauges and 8 accelerometers in the in-line direction. The riser properties are summarized in Table 1 and the test matrix is presented in Table 2. Both bare riser configuration and configurations with partially (50%) and fully (100%) straked coverage were analyzed in the present study.

The data used in the present study are derived from the cross-flow (CF) bending strain gauges along the riser. The fatigue damages rates were assuming Stress Concentration Factor (SCF) of 1.0 and single-slope DNV F2 S-N curve. Some of the measured data from the slow speed 100% straked cases were removed where the RMS was close to the quoted resolution of the instruments (1 micro-strain). It is also noted that one of the data channels was removed due to an error in the strain gauge.

**Table 1 – Riser properties**

Parameter	Dimension
Total length between pinned ends	38.00 m
Outer diameter	27 mm
Wall thickness of pipe	3.0 mm
Bending stiffness, EI	598.8 Nm <sup>2</sup>
Young modulus of pipe, E	3.62 10 <sup>10</sup> N/m <sup>2</sup>
Axial stiffness, EA	8.19 10 <sup>6</sup> N
Mass (air filled), measured	0.761 kg/m
Mass (water filled) estimated	0.933 kg/m
Mass ratio	1.62

**Table 2 - NDP test program**

Riser	Flow config.	# of cases
Bare riser	Shear flow	22 different velocities
Bare riser	Uniform flow	22 different velocities
50% strakes (17.5D / 0.25D)	Shear flow	22 different velocities
50% strakes (17.5D / 0.25D)	Uniform flow	22 different velocities
100% strakes (17.5D / 0.25D)	Shear flow	11 different velocities
100% strakes (17.5D / 0.25D)	Uniform flow	22 different velocities
Total number of cases		121

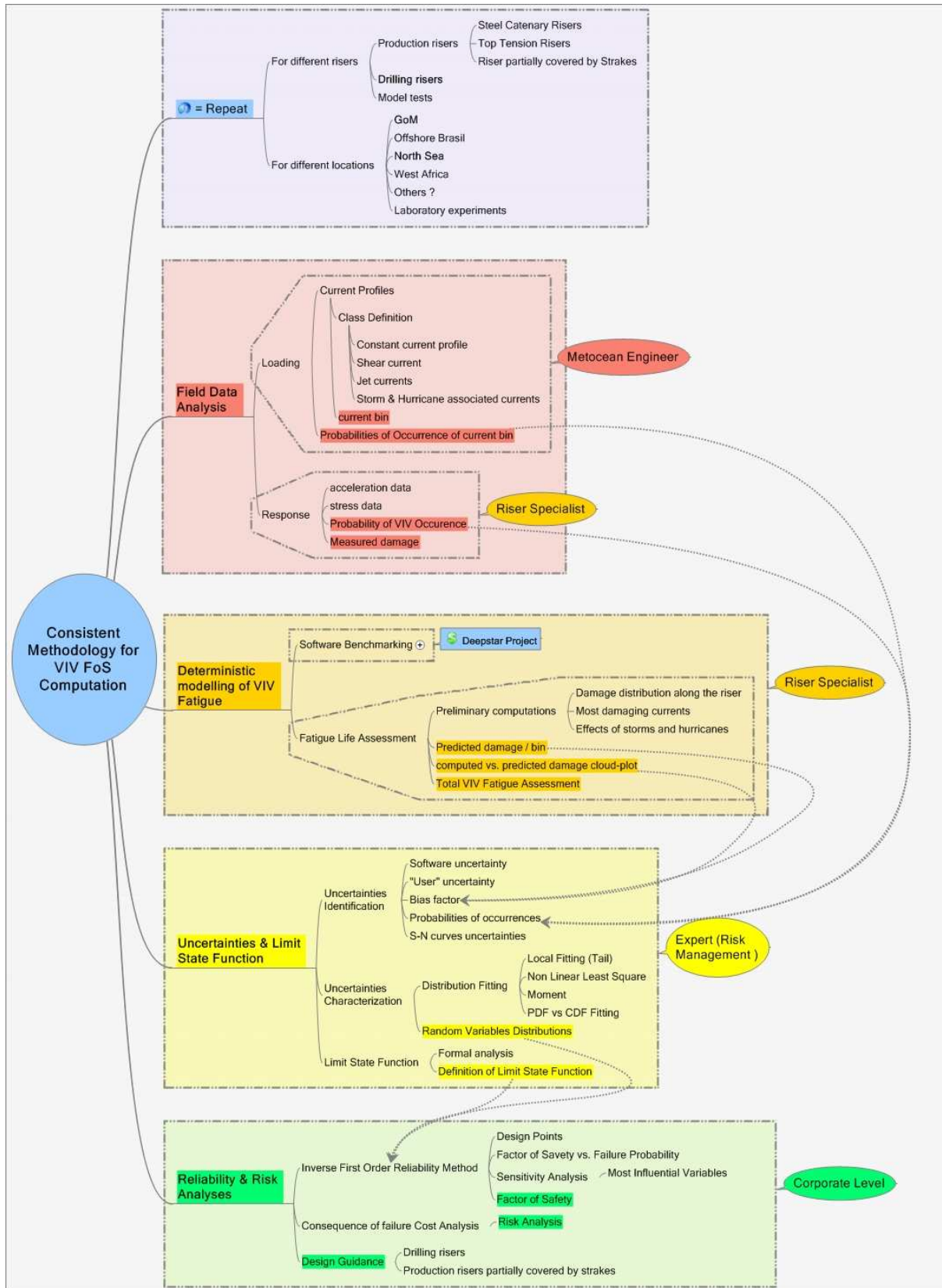


Figure 3: VIV FoS Calibration Methodology

## PREDICTED VS. MEASURED VIV FATIGUE DAMAGE

Step (ii) of the calibration process consists of comparing the computed and measured damage for the considered dataset. The selected cases and data subsets from the NDP test data used in the study are presented in Figure 4. In addition, the uniform current / bare pipe calibration was repeated using just the 1x (fundamental cross-flow frequency) measured response by filtering the higher harmonics.

In the present study, the most commonly used VIV prediction software were used to obtain predictions of the VIV fatigue damage rates. Preliminary computations were performed with:

- SHEAR7v4.5, run by Prof. K. Vandiver;
- VIVAv6.4, run by Prof. M. Triantafyllou; and
- VIVANA v3.7, run by Prof. C.M. Larsen/E. Passano.

Final computations were performed using development versions of the software.

In each software program, the riser was modeled based on the NDP riser configuration as used in the experiments. From these models, the same loading conditions were applied and the VIV fatigue damage rates corresponding to the loading conditions (test cases) were computed (predicted).

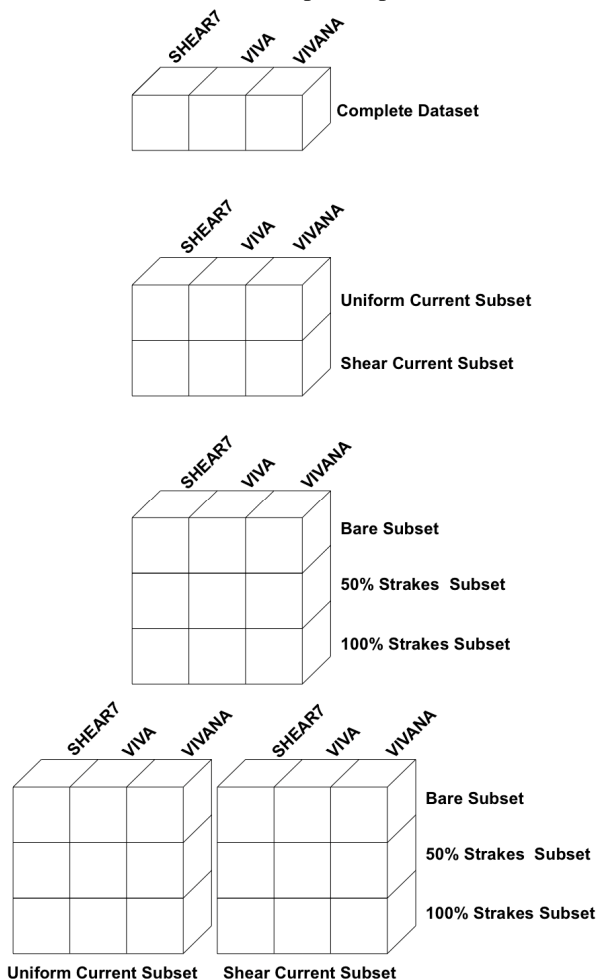


Figure 4: Data Subsets used to estimate the FoS.

The damage rates computed by the VIV software were extracted from the specific locations where the strain gauges were positioned during the experiments. Step (iii) of the calibration procedure consists of plotting the damage scatter plot together with the equality line (i.e. perfect match) for comparison; see Figures 5, 6 and 7 for the bare riser subset.

Hydrodynamic coefficients for the actual strake designs were not available. Since VIVANA requires such data to be explicitly known, coefficients were estimated from results published by Ding et al. [13].

## DISTRIBUTION OF THE BIAS FACTOR

Step (iv) of the calibration procedure consists of filtering and fitting the bias distribution derived from the damage scatter plot. In deriving the probability density functions (PDFs), the data were taken both as a single set, irrespective of the riser configuration and the current profile to which they refer, and partitioned into subsets to assess whether consistent FoS are obtained for each individual riser configuration. Data subsets for bare, 50% and 100% straked riser configurations placed in uniform or sheared current profiles were considered separately (see Figure 4).

Distinctions were also made regarding which piece of software and which analysis parameters (distribution fitting technique) were used in generating the predicted results for use in determining the bias PDF. It is indeed important to make sure that the choice of the fitting process for the PDF does not significantly affect the FoS, as the calibration process would then not be reliable.

### Distribution fitting

As the bias factors generally exhibit a large scatter, it was found more appropriate to consider the PDF of  $\ln(\alpha)$ . Figures 8 and 9 show two examples. Different techniques were used to fit the obtained PDF. With this choice of variable, fitting the PDF by a Gaussian curve is actually equivalent to  $\alpha$  following a log-normal distribution. For experimentally-derived PDFs with multiple peaks, a double Gaussian distribution and a kernel-based estimation were also used.

### Filtering using damage threshold

As measurements were obtained all along the riser length, some experimental data points exhibit high damage rates while others exhibit very low rates. The question was therefore raised whether the data points with low damage should be given the same weight as the data points with high damage when deriving the FoS. The use of the damage threshold was introduced to carefully study the influence of the data points used in the analysis. The damage threshold,  $p$ , is defined such that for  $p = 0.1$  only the top 10% of the data points with the highest measured damage were retained to derive the bias distribution and to compute the FoS. For  $p = 1$ , all the data points were retained to fit the bias distribution and derive the value of the FoS. A filtering process therefore occurs as the damage threshold is decreased. The lower the damage threshold, the higher the weight of the data points where high damage were

measured. However, size of the sample is decreasing so that there is a practical limit below which it is not possible to derive FoS values for small  $p$  values (typically 5% in the present case).

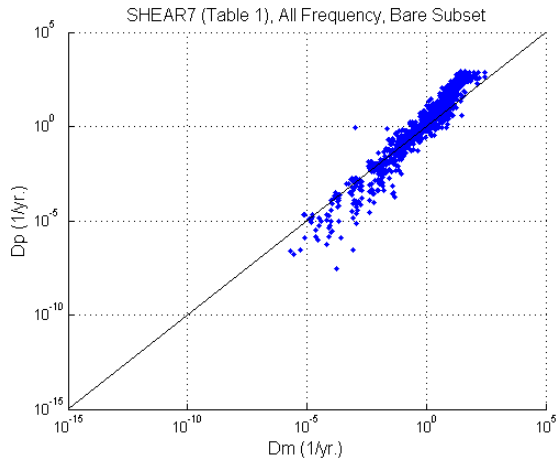


Figure 5: SHEAR7 scatter damage plot – Bare riser

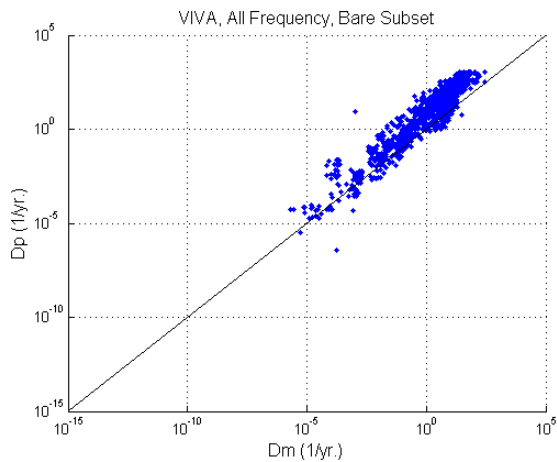


Figure 6: VIVA scatter damage plot – Bare riser

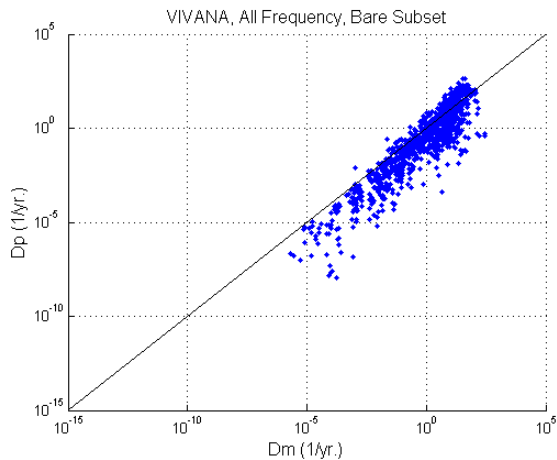


Figure 7: VIVANA scatter damage plot – Bare riser

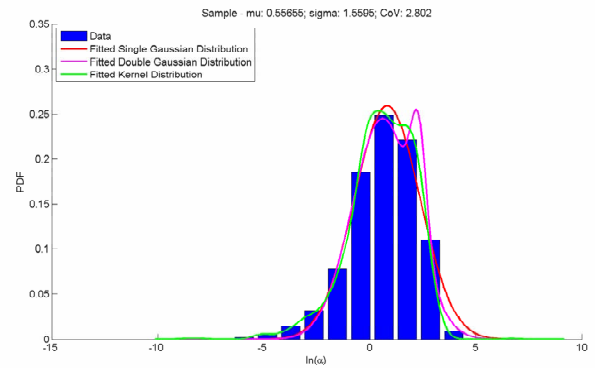


Figure 8: SHEAR7 Scatter – Bare riser Subset

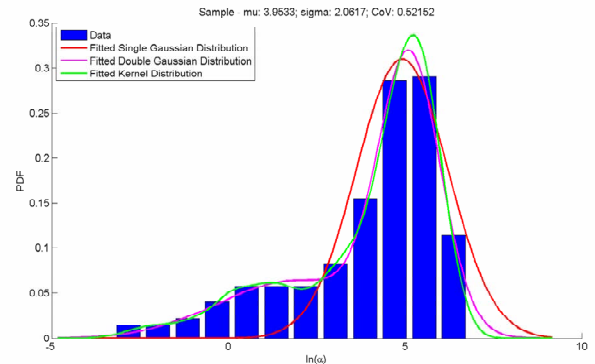


Figure 9: SHEAR7 Scatter – Fully straked riser Subset

## RESULTS ANALYSIS

Prior to analyzing the results, it should be noted that the FoS values derived in the study are not to be taken as general or definitive FoS due to the limitation of the single-event limit state function. The single-event limit state function was constructed to include statistical characterization of the fatigue prediction bias, but refers only to the fatigue damage due to a single event. Previous studies [1] have shown that the use of the complete limit state function, instead of the simplified one, leads to smaller values of the FoS to meet a given level of reliability as the uncertainty is spread over a range of current conditions. The values presented hereafter are illustrative for a probability of failure of  $10^{-3}$ .

The FoS obtained on each riser configuration (bare, 50% straked and fully straked) in uniform and shear currents using SHEAR7, VIVA and VIVANA are plotted in Figures 10 to 21 against  $p$ , the damage threshold. Different symbols are also used depending on the distribution fitting process.

The results indicate sensitivity of the FoS to riser configuration (bare / partially-straked / fully-straked), type of environmental loading (uniformed current / sheared current), i.e. location dependent, VIV software used to perform the fatigue analysis, and parameters intrinsic to the calibration process such as the fitting technique and the damage threshold.



Since we are more concerned with areas of high damage rate, FoS values for lower damage threshold ( $p$ ) are of most interest. FoS values in this range are more consistent, but vary widely from configuration to configuration. Obviously using a single global FoS, as is normally done, does not appear optimal.

### **Effect of fitting technique and filtering**

First, it is important to understand how the obtained FoS varies with the parameters related to the calibration process. If the FoS values were too sensitive with regard to the distribution fitting or the filtering processes, this would be a serious limitation to the proposed methodology but the results hereafter confirm that this is not the case as consistent values of the FoS are obtained.

Generally, the use of the double Gaussian or kernel-based distributions allows better representations of the tails of the distributions compared to the single Gaussian which tends to fit the body of the distribution but usually under-estimates the tail of the PDF. As the failure design point lies in the tail region, the kernel-estimate and the double-Gaussian method should provide a better FoS estimate. Comparing the FoS values obtained with single and double Gaussian would show if the single Gaussian fitting is a realistic approximation. If not, then the kernel-based estimate is most probably the best approximation. It should also be noted that discerning where to center the second Gaussian distribution is not always obvious, as the PDFs sometimes do not clearly exhibit two well-separated peaks. When this was the case, the double Gaussian fitting was not used. The kernel-based distribution, which involves a number of Gaussian distributions, is therefore the preferred fitting technique.

As a general trend, it is observed that FoS tend to decrease with the damage threshold, indicating that the error is generally less for data points associated with high damage values, thus the interest of using the damage threshold. In other words, as more data points with lower damage are included in the analysis, the coefficient of variation (a measure of the relative scatter in the data) is observed to increase, thus the FoS. From a practical point of view, the data points with the highest damage are more important as failure is expected to arise at these locations first. These points should therefore be given a higher weight when estimating the FoS. Thus, values of the FoS for small  $p$  values will therefore be considered in the following.

From the last two sections, it is concluded that the fitting and filtering processes that have been proposed are satisfactory for the purpose of calibrating as they provide consistent and robust estimations of the FoS.

### **Effect of riser configuration and current loading**

For a given software, the obtained values of the FoS vary over a large range depending on the riser configuration (bare, partially and fully straked) as can be seen by comparing Figures 10, 13 and 16 for SHEAR7, Figures 11, 14 and 17 for VIVA and Figures 12, 15 and 18 for VIVANA. All these figures were obtained for a constant probability of failure equal to  $10^{-3}$ .

This suggests that it is more appropriate to define VIV FOS for a specific type of current loading and a specific riser configuration, instead of defining a general VIV fatigue FoS for a given VIV prediction software. In practical application, the FoS sensitivity is expected to be extended to include the type of riser (drilling riser / permanently installed riser), the location and the target probability of failure of the equipment.

### **Effect of riser software**

FoS also depends on the VIV software that has been used to performed the analysis. For the bare riser case in uniform current, the FoS for SHEAR7 and VIVA is between 2 and 10. Similar values are obtained for the 50% and 100% straked configurations. VIVA seems to be very conservative for 100% straked configuration in uniform current. The VIVANA program gives a significant under prediction of the response for a number of cases, both for bare pipe and models with strakes.

### **Effect of higher harmonics**

It is noted that the VIV prediction programs only compute the cross-flow riser damage at the first harmonic, i.e. at the Strouhal frequency while the observed responses show some contributions from higher harmonics. The latter are not included in the VIV damage that is predicted, but are present in the so-called “measured” damage. This disparity is precisely to be included as part of the FoS that is to be applied to the predicted damage.

An analysis was performed with respect to the uniform-flow / bare riser data subset to assess the FoS when the measured damage computation was performed using only the 1x contribution instead of all the CF harmonics. The resulting measured VIV fatigue damage rates are lower and the FoS values obtained are an order of magnitude lower than the values obtained using all the CF harmonics.

## **PROPOSED APPLICATION**

The above methodology when applied using VIV field measurements together with associated met-ocean conditions (current profile and probabilities) at that location and the full limit state function allows derivation of the specific FoS for that configuration at that location. The application of this methodology to drilling risers in different locations (GoM and North Sea) is presented in [8].

The more complete limit state function (multiple-event limit state function which considers the weighted summation of fatigue damage over all current profiles expected at a site during a typical year) results in more practical FoS values. The multiple-event limit state function, however, was not used in the present study since the experimental data does not have the required probabilistic description of the current conditions. The single-event limit state function, however, gives an indication of how VIV fatigue FoS should be determined.

From a project perspective, it is interesting to perform this calibration exercise even a posteriori, i.e. when full-scale data from the installed risers becomes available. Full-scale measurements of the accelerations (preferably with co-located

angular rates) together with associated current profiles are the required input data. It should also be noted that the tools have now been developed to largely automate the calibration process as it essentially consists of processing the data and running the simulation in a batch mode. The main result is then the level of conservatism inherent to the design. The information can then be reused for new build risers.

## CONCLUSIONS

VIV of risers has been studied extensively over the last fifteen years. It is now time for the offshore oil/gas industry to benefit from this accumulated knowledge to reduce operators CAPEX/OPEX costs due to overly conservative VIV predictions whilst ensuring that there is a rational basis for FoS selection. This paper presents a demonstration of the FoS calibration methodology [1] applied on medium scale VIV data. Namely, it demonstrates the utilization of established reliability analysis methods to cast VIV FoS in the context of a meaningful probability of failure based on NDP medium-scale test data.

The model test experiments on a well-instrumented 38m length riser are considered to be state-of-the-art VIV data. The experiments were simulated using different VIV software currently used in the industry, namely SHEAR7, VIVA and VIVANA. The experimental results were provided prior to running the simulations. The only constraint that was enforced on the software input parameters was to use a single set of parameters for each riser configuration (bare, partially or fully straked), as would be the case for studying a real riser configuration during design. The human/user component was removed from the study as the most expert users of the software supervised the simulations. The following conclusions were drawn from the study:

- The study suggests that the idea of utilizing a single global VIV FoS may not be appropriate.
- The study indicates sensitivity of the FoS to:
  - Riser configuration (bare / partially-straked / fully-straked).
  - Type of environmental loading (uniformed current / sheared current), i.e. location dependent.
  - VIV software used to perform the fatigue analysis.
- It seems more appropriate to define FoS for a specific riser configuration for a given VIV prediction software. The study shows that the FoS defined for all configurations is not appropriate due to different partitions of the data not grouping well.
- In practical applications, the FoS is expected to also be sensitive to the type of riser (drilling riser / permanently installed riser) and the target probability of failure of the equipment.

This exercise, funded by the DeepStar consortium, demonstrates an approach to computing a reliability-based FoS using model-scale VIV data. Subject to availability of full-scale data, the approach can be performed for full-scale applications where practical and meaningful FoS can be defined for the

industry. Future work will involve the more complete limit state function (multiple-event limit state function), which considers the weighted summation of fatigue damage over all current profiles expected at a site during a typical year, resulting in more practical FoS values.

## ACKNOWLEDGEMENT

The authors would like to acknowledge the financial support from DeepStar Phase IX. The Norwegian Deepwater Program (NDP) is also acknowledged for providing access to all the results of the MARINTEK experiments on the 38m long riser models. The authors would also like to thank M. Santosa (AMOG Consulting) who performed the analyses under supervision.

## REFERENCES

- [1] Chaplin, Bearman, Cheng, Fontaine, Graham, Herfjord, Hueru Huarte, Isherwood, Lambrakos, Larsen, Meneghini, Moe, Pattenden, Triantafyllou, Willden (2005) "Blind predictions of laboratory measurements of vortex-induced vibrations of a tension riser", *Journal of Fluids and Structures*, Vol. 21, pp. 25-40.
- [2] Bearman, Chaplin, Fontaine, Graham, Herfjord, Hueru, Lima, Meneghini, Schulz, Willden (2006) "Comparison of CFD Predictions of Multi-Mode Vortex-Induced Vibrations of A Tension Riser with Laboratory Measurements", *Proc.6th Intern. Symposium on FSI, AE & FIV: ASME PVP Division Summer Meeting, Vancouver, BC, Canada, July 23 – 27*.
- [3] Marcollo, Vandiver & Chaurasia, 2007, "Phenomena Observed in VIV Bare Riser Field Tests", *26th International Conference on Offshore Mechanics and Arctic Engineering, OMAE2007-29562*.
- [4] Trim, Braaten, Lie and Tognarelli (2005), "Experimental investigation of vortex-induced vibration of long marine risers", *Journal of Fluids and Structures*.
- [5] Tognarelli, Taggart, Campbell (2008) "Actual VIV Fatigue Response of Full Scale Drilling Risers: With and Without Suppression Devices", *27th International Conference on Offshore Mechanics and Arctic Engineering, OMAE2008-57046*.
- [6] Vandiver, Swithenbank, Jaiswal & Marcollo, 2006, "The Effectiveness of Helical Strakes in the Suppression of High-Mode Number VIV", *Offshore Technology Conference, OTC 18276. Winner of IPTI - LUBINSKI Best Paper Award*.
- [7] Leira, B., Meling, T., Larsen, C.M., Berntsen, V., Stahl, B. and Trim, A. 2005. "Assessment of Fatigue Safety Factors for Deep-Water Risers in Relation to VIV". *Journal of Offshore Mechanics and Arctic Engineering*, Nov 2005, Vol. 127 pp353-358.
- [8] Tognarelli, M., Fontaine, E., Beynet, P., Santosa, M., Marcollo, H., (2010). "Reliability-Based Factors of Safety for VIV Fatigue Using Field Measurements" *Proc. 29th Int'l Conf. Ocean, Offshore & Arctic Engrg. ASME. OMAE2010-21001*.
- [9] Braaten, H. & Lie, H., (2004). "NDP Riser High Mode VIV Tests Main Report". Norway. MARINTEK. Report No. 512394.00.01.

[10] Det Norske Veritas. (2005). "Recommended Practice – Riser Fatigue". DNV-RP-F204.

[11] Tognarelli, M., Gabbai, R. & Campbell, M. (2009). "An Approach to Include Observed VIV Likelihood in Drilling Riser Fatigue Analyses." Proc. 28th Int'l Conf. Ocean, Offshore & Arctic Engrg. ASME. OMAE2009-79443

[12] Melchers, R.E. (1987). "Structural Reliability Analysis and Prediction", Ed. Ellis Horwood.

[13] Ding, Z.J., Balasubramanian, S., Lokken, R.T and Yung, T-W.: "Lift and damping characteristics of bare and straked cylinders at riser scale Reynolds numbers" Offshore Technology Conference, OTC16341, 2004

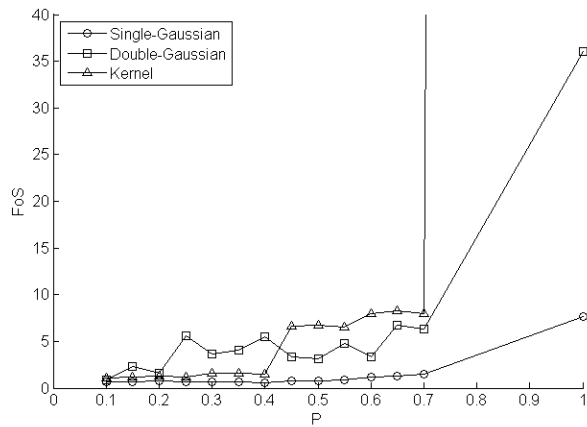


Figure 10: SHEAR7 – Bare Riser Uniform Current

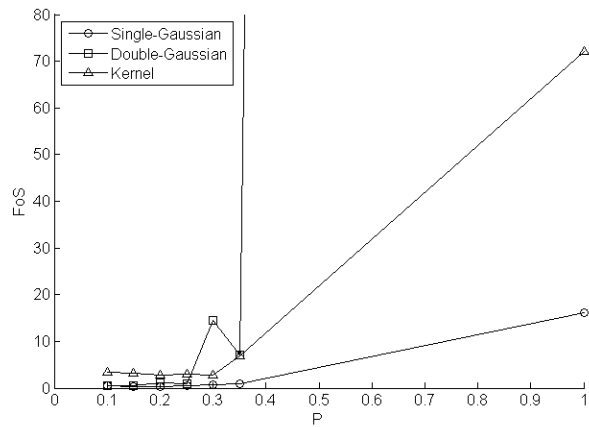


Figure 13: SHEAR7 – 50% straked Uniform Current

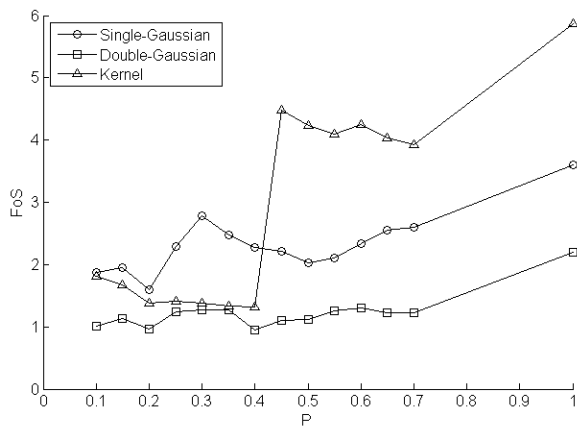


Figure 11: VIVA – Bare Riser Uniform Current

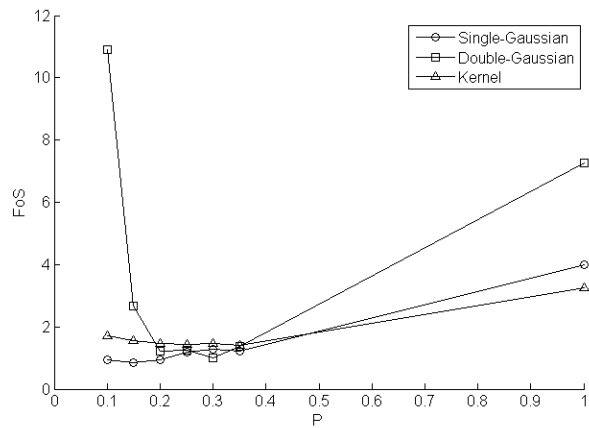


Figure 14: VIVA – 50% straked Uniform Current

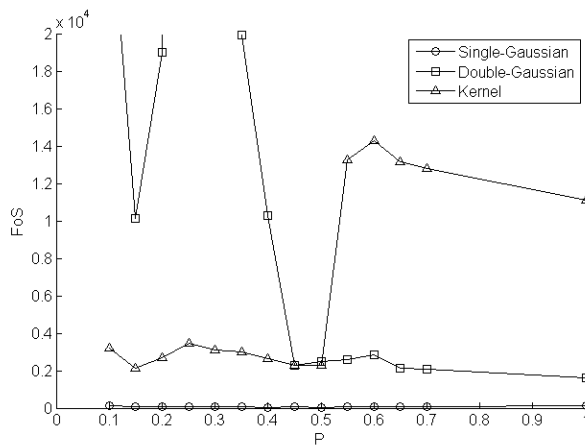


Figure 12: VIVANA – Bare Riser Uniform Current

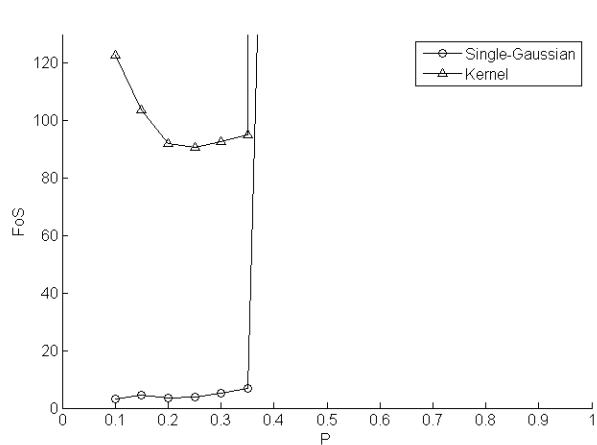


Figure 15: VIVANA – 50% straked Uniform Current

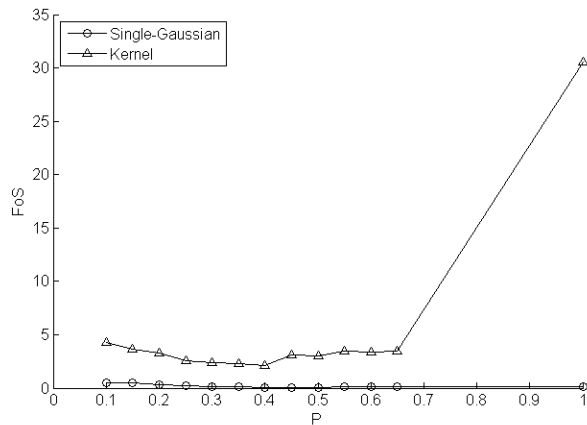


Figure 16: SHEAR7 – 100% straked Uniform Current

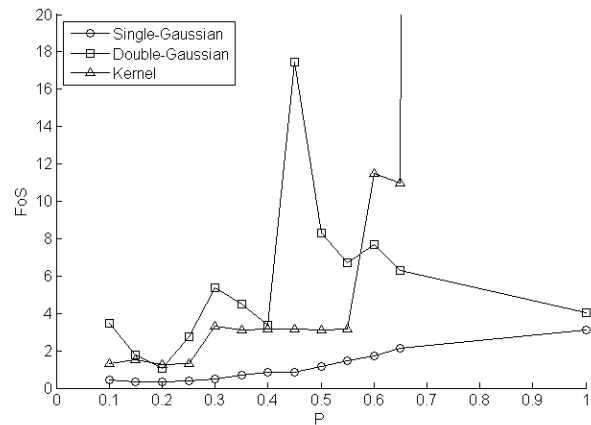


Figure 19: SHEAR7 – 50% straked Shear Current

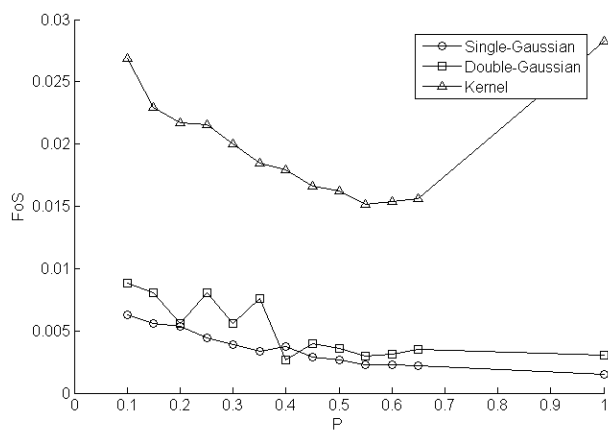


Figure 17: VIVA – 100% straked Uniform Current

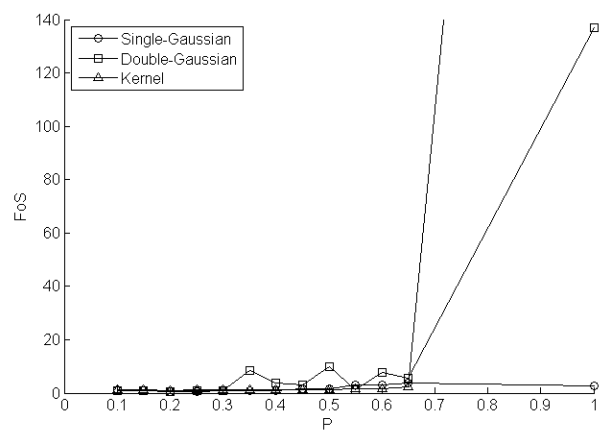


Figure 20: VIVA – 50% straked Shear Current

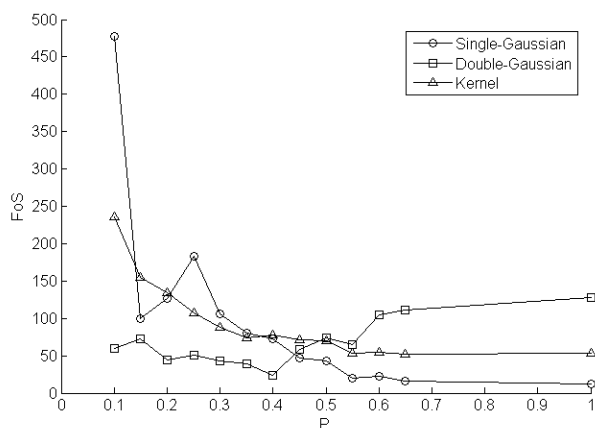


Figure 18: VIVANA – 100% straked Uniform Current

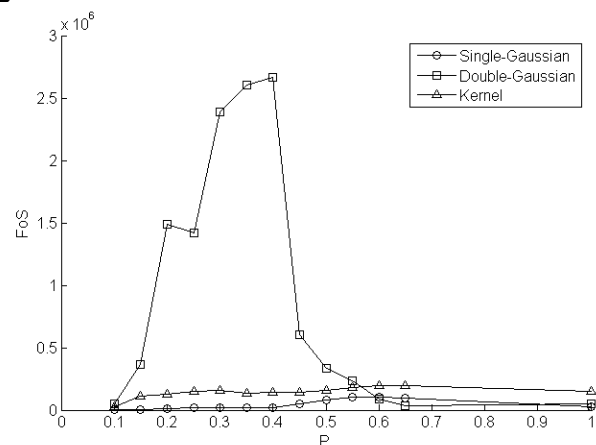


Figure 21: VIVANA – 50% straked Shear Current